IEEE Access
Multidisciplinary ⋮ Rapid Review ⋮ Open Access Journal

Received February 7, 2020, accepted February 24, 2020, date of publication March 4, 2020, date of current version March 13, 2020.

Digital Object Identifier 10.1109/ACCESS.2020.2977562

Multiband and Photonically Amplified Fiber-Wireless Xhaul

EDUARDO SAIA LIMA[1], RAMON MAIA BORGES[1,2], LUIZ AUGUSTO MELO PEREIRA[1], HUGO RODRIGUES DIAS FILGUEIRAS[1], ANTÔNIO MARCOS ALBERTI[3], AND ARISMAR CERQUEIRA SODRÉ, JR.[1]

[1]Laboratory WOCA, National Institute of Telecommunications (Inatel), Santa Rita do Sapucaí 37540-000, Brazil
[2]Federal University of Itajubá, Itajubá 37500-903, Brazil
[3]ICT Laboratory, National Institute of Telecommunications (Inatel), Santa Rita do Sapucaí 37540-000, Brazil

Corresponding author: Arismar Cerqueira Sodré, Jr. (arismar@inatel.br)

This work was partially supported by Rede Nacional de Ensino e Pesquisa (RNP), with resources from Ministério da Ciência, Tecnologia, Inovação e Comunicações (MCTIC), Grant No. 01250.075413/2018-04, under the Radiocommunication Reference Center (Centro de Referência em Radiocomunicações-CRR) project of Inatel. The authors thank the financial support from Coordenação de Aperfeiçoamento de Pessoal de Nível Superior (CAPES), Financiadora de Estudo e Projetos (FINEP), Fundação de Amparo à Pesquisa do Estado de Minas Gerais (FAPEMIG), Conselho Nacional de Desenvolvimento Científico e Tecnológico (CNPq) and Keysight Technologies.

ABSTRACT We propose and report the implementation of a multiband and photonically amplified fiber-wireless (FiWi) Xhaul based on radio over fiber (RoF) technology and four-wave mixing (FWM) nonlinear effect, aiming 5G applications. The proposed ultra-wideband approach enables to simultaneously transport and amplify multiple radiofrequency (RF) signals through optical links, which might be employed as backhaul, midhaul or fronthaul of cellular systems. The FWM effect, originated from the use of 35-m highly nonlinear fiber piece, gives rise to RF gain, when compared to conventional RoF (CRoF) systems. We demonstrate our technique allows replacing two conventional RF amplifiers with enhanced digital performance and/or significantly increasing the system throughput in 2.4 times, attaining 12 Gbit/s. Furthermore, a dual-band (7.5 and 28.0 GHz) wireless fronthaul, preceded by a 12.5-km optical midhaul, illustrates the multiband and photonically amplified FiWi Xhaul, by means of providing performance in terms of root mean square error vector magnitude (EVM_{RMS}) in accordance to the 3GPP recommendations and at low phase noise level.

INDEX TERMS 5G networks, four-wave mixing, microwave photonics, optical-wireless networks.

I. INTRODUCTION

International mobile telecommunications (IMT) for 2020 and beyond claims for a physical layer network review, as well as the use of innovative technical solutions to fulfill the next generations scenarios and tough requirements. Particularly, the fifth generation of mobile networks (5G) conceives Gbit/s throughput, reliable mobility, low latency and user experience continuity toward human and machine-centric applications [1]. 5G is going to take advantage of new waveforms, high-performance antennas, additional spectrum bands including millimeter-waves (mm-waves) and massive multiple-input multiple-output (mMIMO) techniques [2]–[5]. In parallel, trends on network planning point out to optical-wireless convergence and mobile dense heterogeneous networks (HetNet), which consist of a mix of cell sizes with simultaneous radio access technologies (RATs) and the integration of backhaul (BH) and fronthaul (FH) into a common transport network called Xhaul [6]–[8]. As a consequence, the radio access network (RAN) should evolve towards creating unprecedented levels of flexibility to the software layer, allowing virtual network functions to be performed anywhere from cloud to the edge. In this way, future RANs are going to be aligned with the imminent increase on the number of the HetNet base stations (BS) [9], as well as cloud-based resources.

In distributed RAN (D-RAN), the baseband unit (BBU) is physically located with the remote radio unit (RRU) in BSs. On the other hand, cloud/centralized RAN (C-RAN) keeps RRU close to the antenna and displaces BBUs from the remote cell sites to a unified central office (CO), giving rise to the BBU pool concept. In such a way, the BBU pool can be directly connected to diverse RRUs, by using FH as a physical link, which is mostly based on single-mode fibers

The associate editor coordinating the review of this manuscript and approving it for publication was Tariq Umer.

(SMFs). Another typical way to connect BBUs and RRUs on C-RAN is employing an optical midhaul (MH) up to a distribution unit (DU), followed by wireless and/or optical FHs. C-RAN brings the benefits of straight-forward communication among co-located BBUs, reuse infrastructure, simplify network operations and management, support of multiple technologies, reduce energy consumption and lower capital expenditure (CAPEX) and operational expenditure (OPEX), moreover, the network becomes more heterogeneous and self-organizing [9]. Once implemented, the C-RAN will bring other benefits, such as easier and faster network deployments and increased network flexibility.

Microwave photonics (MWP) has been recognized as an important enabler for the emerging broadband and multiband 5G systems, bringing diverse techniques for enhancing the mobile system performance and making the mm-waves use feasible [10]–[12]. Indeed, the photonics technological maturity on broadband radiofrequency (RF) generation and processing has empowered the development of diverse photonics-assisted devices, such as analog-to-digital converters [13], RF filters [13], RF phase shifter [14], RF up and down-converters [13], [15], RF front-ends [16], [17] and RF amplifiers [18]–[21]. Particularly, our research group has intensely worked on photonics-assisted RF amplification in the last years [19]–[21], including a demonstration of constant RF gain up to 27 dB over an ultra-wideband from 300 kHz to 50 GHz [21]. In this context, our main goal is reducing or even eliminating the requirement for broadband high-gain electrical amplifiers at RRU, which impose noise and are challenging/expensive mainly in the mm-waves band. Interference and nonlinear impairments imposed to multiple frequency bands are commonly caused by non-perfectly linear-gain amplifiers [22]. Many investigations in literature and comparisons among multiple photonics-based techniques and electronic-microwave amplifier-stages indicate that the signal degradation comes mainly from the electronic devices [23].

Finally, fiber-wireless (FiWi) systems based on analog radio over fiber (RoF) technology have been considered as a potential candidate for mobile MHs and FHs, as well as an attractive solution over common public radio interface (CPRI), which suffers from significant scalability issues [24], [25]. RoF-based FiWi systems make possible to concentrate most pieces of hardware at the BBU pool and transport multiple RF signals to densely distributed RRUs, exploiting the existing wavelength-division-multiplexing passive optical network (WDM-PON) capillarity [26]. All these features create unprecedented levels of flexibility to deploy higher-layer network functions closer to BBUs in CO.

The current work introduces the concept and reports the implementation of a multiband and photonically amplified FiWi 5G Xhaul based on RoF technology and four-wave mixing (FWM) nonlinear effect. Our main contributions over the state-of-the-art are the following ones: a novel technique for providing photonics-assisted RF amplification using only one laser, replacing two broadband RF amplifiers with enhanced digital performance; a new architecture for photonics-assisted RF amplification, in which the optical pump is coupled after the electro-optic modulation process; the implementation of a dual-band and Gbit/s FiWi 5G Xhaul based on the unprecedented photonics-assisted RF amplification (PAA) technique and architecture, using a dual-drive Mach-Zehnder modulator (DD-MZM).

The manuscript is structured in five sections. Section 2 introduces our concept of multiband and photonically amplified FiWi 5G Xhaul based on RoF and FWM. Section 3 describes the novel photonic-assisted RF amplification technique and reports its experimental characterization as a function of different figures of merit, such as RF gain, phase noise and root mean square error vector magnitude (EVM_{RMS}). Section 4 presents the implementation of the multiband and photonically amplified FiWi Xhaul. Finally, the conclusions and future works are outlined in Section 5.

II. MULTIBAND AND PHOTONICALLY AMPLIFIED FIWI 5G XHAUL BASED ON ROF AND FWM

Fig. 1 illustrates our concept of multiband and photonically amplified FiWi 5G Xhaul based on RoF and FWM, in which the PAA block is located at CO, jointly with the BBU pool. The central office can access DU through optical midhauls or be directly connected to RRU using an optical fronthaul. In this way, X-haul links in conjunction with the PAA block could be exploited for simultaneously distributing and amplifying multiple cellular signals from diverse telecom operators, aiming to share the infrastructure. The same wavelength might be used for transporting all desired RF signals and/or frequency bands, for instance using dual-driver Mach-Zehnder modulators [26], with the purpose of significantly reducing CAPEX and enhancing the overall system performance. Furthermore, the proposed architecture provides benefits for the IMT system software layers, since it enables physical/link layer functional splitting, such as the separation of the user and control planes in higher layers [27]. This functionality allows network functions to be deployed as specialized devices or virtualized as virtual network functions (VNFs) [28], by reason of the PAA block is transparent to higher layers. Depending on the required bandwidth, delay and synchronization, physical/link layer functions can be accomplished in hardware or software. The optimal split can be dynamically achieved by software-based orchestration and control, reacting to changes in traffic load, service requirements and failures. Additionally, software-defined networking (SDN) allows virtualization of physical/link layer resources as a service, i.e. through computer programs [29]. Applications in the upper layers can request slices of network, processing and storage resources, creating customized slices of network functions and transport in Xhaul. In other words, the optimal physical/link layer functional splitting can be performed as a function of the 5G vertical, since requirements are very different. As a conclusion, it becomes feasible an

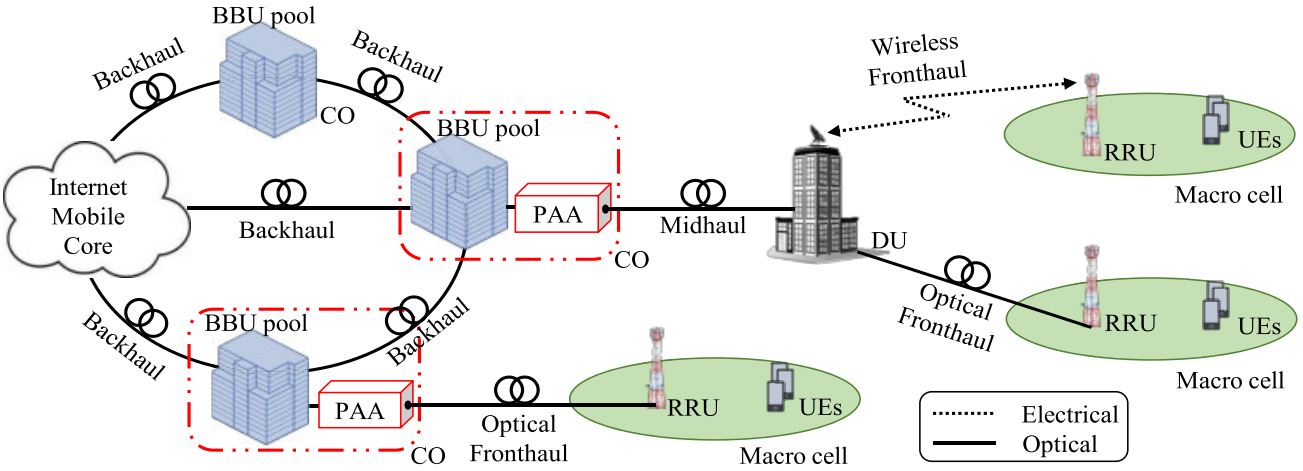

FIGURE 1. Multiband and photonically amplified fiber-wireless Xhaul: BBU- baseband unit; RRU- remote radio unit; PAA- photonics-assisted RF amplification; UE- user equipment.

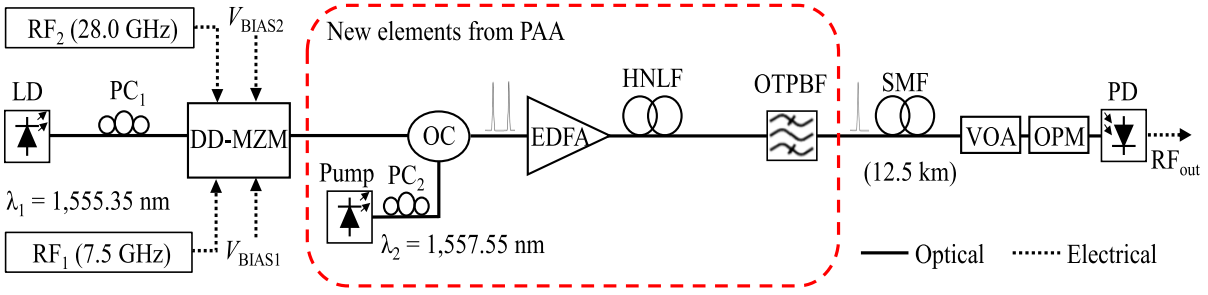

FIGURE 2. Proposed photonics-assisted amplification technique architecture: RF_1- 7.5 GHz electrical driven-signal; RF_2- 28.0 GHz electrical driven-signal; LD- laser diode; PC_1- polarization controller 1; DD-MZM- dual-drive Mach-Zehnder modulator; PC_2- polarization controller 2; OC- optical coupler; EDFA- erbium-doped fiber amplifier; HNLF- highly nonlinear fiber; OTPBF- optical tunable passband filter; SMF- single mode fiber; VOA- variable optical attenuator; OPM- optical power monitor; PD- photodetector.

optimal combination of network function virtualization (NFV), SDN and C-RAN, with the purpose of providing flexibility and robustness. The traffic from BBU pools can be dynamically directed to proper VNFs via NFV orchestration and SDN control. Elasticity of network functions accordingly to established slices is also possible, providing load balancing and optimal resource utilization in the software layer.

III. NOVEL PHOTONIC-ASSISTED RF AMPLIFICATION TECHNIQUE

The novel photonic-assisted RF amplification technique differs from the previous ones [16], [18]–[21] mainly due to the concept and validation of a novel photonics-assisted RF amplification technique based on the use of only one optical pump, as schematized in Fig. 2. Moreover, contrary to our previous papers, the optical pump is now continuous (CW), since it is coupled to the data signal after the electro-optic modulation process. One more novelty is the use of a dual-drive Mach-Zehnder modulator for simultaneously amplifying two distinct frequency bands. Nevertheless, it continues to exploit the four-wave mixing nonlinear effect for photonically amplifying RF signals, from baseband to extremely high frequency (EHF).

A laser diode (LD) generates an optical carrier at $\lambda_1 = 1,555.35$ nm, which is modulated at 7.5 and 28.0 GHz using a DD-MZM. Both bias voltages (V_{BIAS1} and V_{BIAS2}) are properly set between quadrature and null points for optimizing the photonics-assisted RF gain. An optical coupler (OC) is then used to combine the modulated optical carrier with a single continuous pump at $\lambda_2 = 1,557.55$ nm. An erbium-doped fiber amplifier (EDFA) amplifies both wavelengths and launches them into a highly nonlinear fiber (HNLF) for generating FWM products. The HNLF main parameters are the following: length $L = 35$ m; zero-dispersion wavelength $\lambda_0 = 1,557.00$ nm; attenuation $\alpha = 0.8$ dB/km; dispersion slope $S_0 = 0.023$ ps/nm^2/km; nonlinear coefficient $\gamma = 28$ W^{-1}km^{-1}; effective area $A_{eff} = 8.9\ \mu$m^2. It is important to highlight differently to our previous works [19]–[21], in which hundreds of meters of HNLF had been used, we have applied only a short HNLF piece of 35 m, with the aim of avoiding the stimulated Brillouin scattering (SBS) effect and, consequently, maximizing the FWM efficiency.

An optical tunable passband filter (OTPBF) selects the first left FWM product ($\lambda_3 = 2\lambda_1 - \lambda_2$), due to the higher correlation with the modulated carrier in comparison with the first right FWM product ($\lambda_4 = 2\lambda_2 - \lambda_1$). Such higher

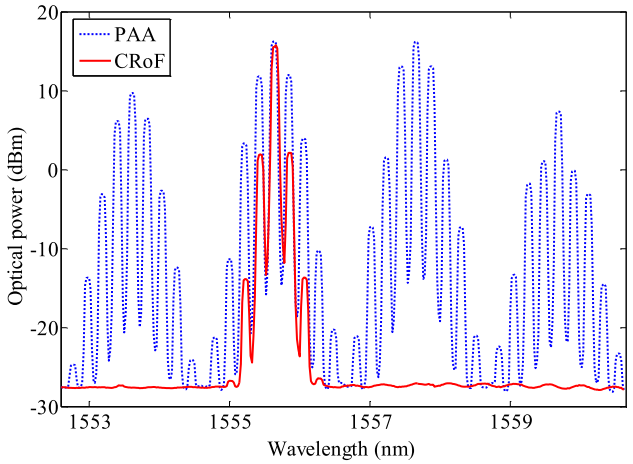

FIGURE 3. Comparison between PAA and CRoF spectra.

correlation is due to the fact only λ_1 is modulated, contrarily to λ_2 that is continuous. The selected product is launched into a single mode-fiber-based 12.5-km dual-band optical Xhaul. A variable optical attenuator (VOA) and an optical power monitor (OPM) are used for controlling and measuring the optical power level at the photodetector (PD) input, respectively, which performs the optical-to-electrical conversion (O/E) of both RF signals.

The photonic-assisted RF amplification [19]–[21] provides higher RF power level (RF_{out}) and signal-to-noise ratio (SNR) improvement, when compared to a conventional RoF (CRoF) system at the same optical power. It is worth highlighting we have used an EDFA not only for compensating the optical losses, but also to increase the optical power level at the HNLF input for stimulating FWM effect and enhancing its efficiency. Only using EDFA would boost the optical power and, consequently, the electrical one. However, the high optical power level could saturate and even damage photodetector, since its maximum allowed power is typically from 0 to 2 dBm. For example, Urick *et al.* [30] proposed a technique based on the use of two optical amplifiers and high-power and expensive photodetectors, whereas our approach only add a piece of HNLF and one optical amplifier. Therefore, the PAA use enables to provide photonics-assisted RF gain at low-level optical power for making possible to use low-cost conventional photodetectors.

The photonics-assisted RF gain is defined as the RF power level between PAA and CRoF for the same optical power. Fig. 3 presents the optical spectra comparison between PAA and CRoF. One can note at the HNLF output multiple FWM products and their respective sidebands separated by 28.0 GHz (RF_2). The sidebands from the 7.5 GHz signal (RF_1) could not be visualized due to the optical spectrum analyzer (OSA) minimum resolution, which is 0.07 nm. By analyzing Fig. 3 as a function of the number of sidebands and their power level, it becomes clear the photonics-assisted RF gain dependence with the FWM efficiency and modulation index (MI). Our research group has been working in reducing the PAA required power level in the last 04 years [16], [19]–[21] and already made a significant progress. In our publication [16] the PAA required optical power was around 23 dBm, whereas in the current paper was 20 dBm. Our main goal is enhancing the technique, as well as using higher-performance components, for eliminating EDFA.

TABLE 1. Optical and electrical power levels.

Setup Stage	Value
RF_1 power (dBm)	14
RF_2 power (dBm)	14
Laser power (dBm)	12
Pump power (dBm)	-15 to 10
Bias voltage 1 (V)	0.8
Bias voltage 2 (V)	1.5

The novel photonic-assisted RF amplification technique characterization has been performed as a function of the system transmission parameters, including the two RF signals power levels, laser and pump optical power levels and DD-MZM bias voltages. Table 1 summarizes the best-obtained set of parameters for maximizing the RF gain and minimizing phase noise, ensuring 20-dBm optical power at the HNLF input.

The first PAA characterization step consisted on implementing a dual-band optical midhaul [31] with photonics-assisted RF gain, aiming to simultaneously transmit a modulated signal at 7.5 GHz and a continuous wave signal at 28.0 GHz in order to evaluate the digital performance in the lower frequency band in the presence of the higher frequency band. One of the key features for the future X-haul networks is the extremely throughput demand from 5G wireless access networks. Aiming this context, the novel PAA approach has also been evaluated using a 2-GHz bandwidth RF signal at 7.5 GHz, as reported in Fig. 4(a). The photonic-assisted RF amplification provides approximately 19 dB flat gain for the entire broadband digital signal with 2 Gsymb/s, without distortions and noise floor increment. Complementary, we have investigated the system phase noise, which is a key parameter for electrical oscillators, as well as photonics-based RF generation and processing. The presence of high phase noise in communication systems degrades the digital performance due to random phase variations. Fig. 4(c) reports the phase noise measurements, which were obtained by using the MXA (N9020A) signal analyzer from Keysight Technologies in the phase noise measurement function. We have measured the phase noise of the vector signal generator (PSG E8267D) and novel PAA approach, which has not increased the system phase noise up to 150 kHz frequency offset. This parameter has increased from 150 kHz to 10 MHz frequency offset, however, it has been kept around −120 dBc/Hz, i.e. keeping low phase noise level.

The optical pump impacts directly in the RF gain, since high optical power levels are necessary for enhancing four-wave mixing products generation. Moreover, the FWM efficiency can be further optimized by setting the laser and

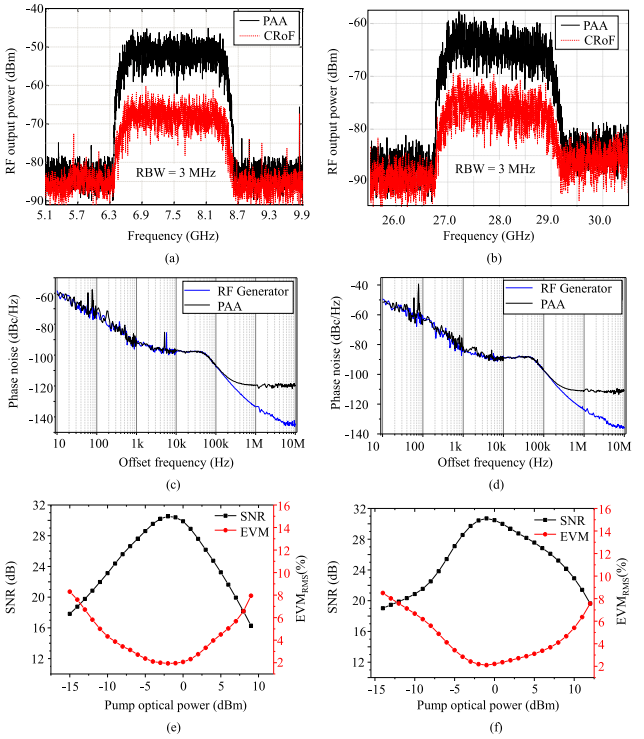

FIGURE 4. **Proposed technique characterization at 7.5 and 28.0 GHz: (a) 2-GHz bandwidth spectra at 7.5 GHz; (b) 2-GHz bandwidth spectra at 28.0 GHz; (c) Phase noise measurement at 7.5 GHz; (d) Phase noise measurement at 28.0 GHz; (e) SNR and EVM_{RMS} as a function of pump optical power at 7.5 GHz; (f) SNR and EVM_{RMS} as a function of pump optical power at 28.0 GHz.**

pump wavelength close to the HNLF zero-dispersion wavelength [32], [33]. Fig. 4(e) reports the digital performance as a function of pump optical power in terms of SNR and EVM_{RMS}, by means of driving DD-MZM with a 4 Gbit/s 16-QAM signal at 7.5 GHz with 0.15 roll-off factor. The modulated signal has been transmitted over 12.5-km optical midhaul and analyzed by using a digital signal analyzer (DSA Z632A). The best results have been obtained from −7 to 3 dBm optical power. Out of this range, EVM_{RMS} increases and SNR decreases due to two distinct reasons: power level lower than −7 dBm results in low FWM efficiency and, consequently, RF gain reduction; for power level higher than 3 dBm, the filtered FWM product power is increased, however, the optical pump power mainly benefits the right side FWM products, which not contributed to RF gain generation.

The second PAA characterization step relied on carrying out the same experiments by applying the modulated signal at 28.0 GHz and a CW signal at 7.5 GHz, with the purpose of investigating the higher frequency band digital performance in the presence of the lower frequency one. Fig. 4 (d) displays the phase noise measurements of PAA and RF generator at 28.0 GHz. The novel photonics-assisted amplification technique has not considerably incremented the residual system phase noise, which has been kept around −112 dBc/Hz. Additionally, 2-GHz bandwidth RF signal spectra have been

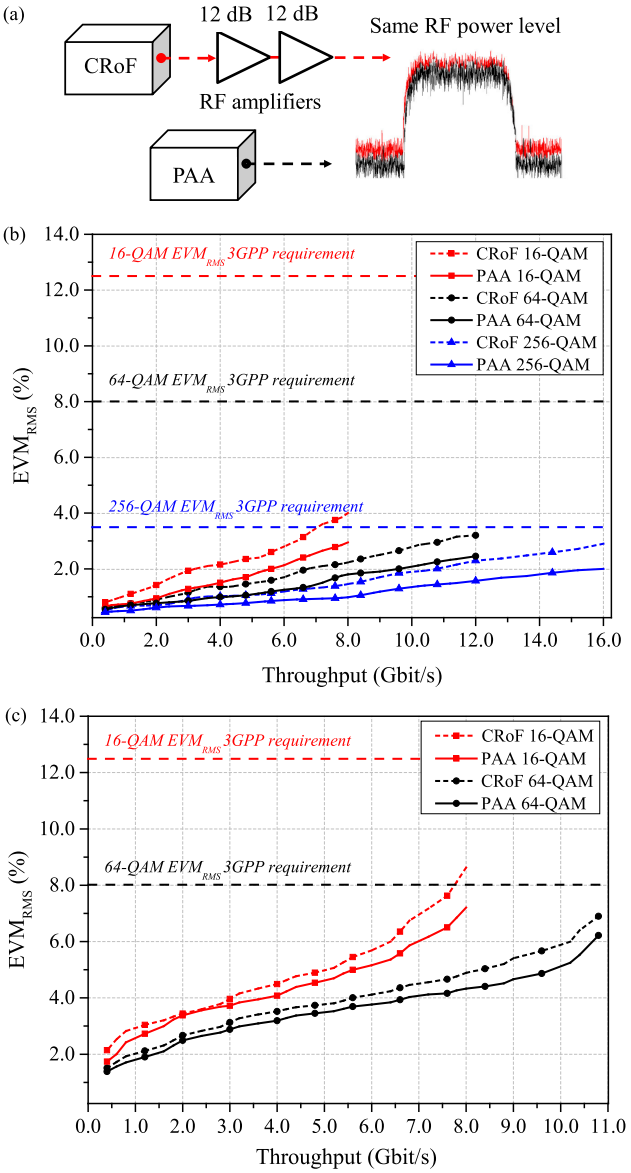

FIGURE 5. **The novel PAA throughput analysis, at the same electrical power, as a function of EVM_{RMS}: (a) block diagram; (b) 7.5 GHz; (c) 28.0 GHz.**

measured in order to evaluate the RF gain in a broadband scenario, as reported in Fig. 4(b). One can note 15 dB amplification for the entire bandwidth. A digital performance has been carried out by analyzing the EVM_{RMS} and SNR as a function of pump optical power for a 3 Gbit/s 64-QAM signal with 0.15 roll-off factor, resulting on 575 MHz occupied bandwidth (Fig. 4(f)). One can observe EVM_{RMS} values below 8.0% and SNR up to 30.6 dB for a pump optical power variation from −13.0 to 12.5 dBm. These results are in accordance to the 3GPP Release 15 specifications [34], [35], namely: EVM_{RMS} below 3.5%, 8.0% and 12.5% for 256-, 64- and 16-QAM, respectively.

The next step on the novel PAA technique characterization was the throughput analysis using the two proposed bands simultaneously, as presented in Fig. 5, and as a function

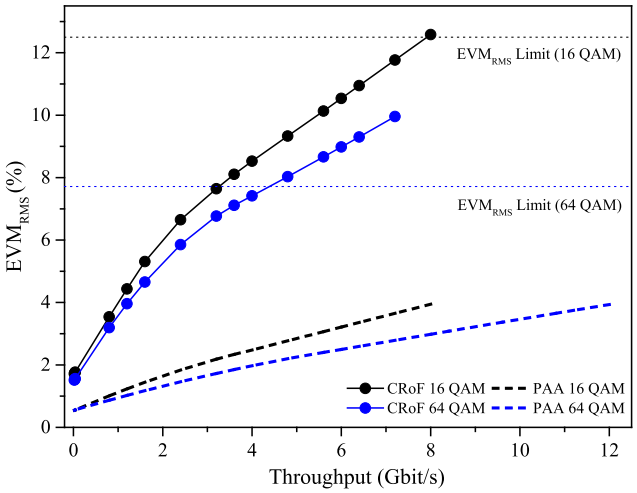

FIGURE 6. The novel PAA throughput analysis as a function of EVM_{RMS} with the same RF front-end.

of the 3GPP Release 15 specifications. Conventional purely electrical RF amplifiers, with 24-dB total gain, have been added to the CRoF system output for comparison purposes as presented in Fig. 5 (a). In this way, the novel PAA technique and CRoF have been properly compared approximately at the same RF power level. At 7.5 GHz (Fig. 5(b)), we have transmitted 16-, 64- and 256-QAM signals, which resulted in 8.0, 12.0 and 16.0 Gbit/s throughput, respectively. One can observe an enhanced digital performance for PAA in all cases, due to its remarkable advantage of photonically amplifying the RF signal without adding noise. Similarly, throughput up to 8.0 and 10.9 Gbit/s with superior performance has been enabled by using the novel PAA technique for simultaneously distributing and amplifying 16 and 64-QAM signals at 28.0 GHz (Fig. 5(c)), respectively. The 3GPP recommendation in terms of EVM_{RMS} has been attained in all evaluated cases. As a conclusion, the novel PAA technique might be considered potential for either reducing the number of RF amplification stages or eliminating purely electrical RF amplifiers in optical Xhauls.

Finally, the system throughput enhancement was properly validated in the 7 GHz band, by means of removing the conventional RF amplifiers from the CRoF and comparing it to PAA at the same photodetected optical power. As expected, PAA provided 19-dB RF gain over CRoF, which implied in improved SNR and, consequently, higher throughput, as reported in Fig. 6. One can note the CRoF system reaches the 3GPP EVM_{RMS} limit at approximately 8 and 4.9 Gbit/s for 16- and 64-QAM, respectively. By using the PAA topology, throughput was increased up to 8 Gbit/s for the 16-QAM and 12 Gbit/s for 64-QAM, which resulted in 2.4 times increment for the higher modulation order. Even though both topologies have enabled the same throughput operating with 16-QAM, it is important to highlight PAA has reduced the EVM_{RMS} from 12.5% to 4%, thus it would be capable to provide even higher throughput in case the bandwidth would be further increased.

IV. DUAL-BAND AND PHOTONICALLY AMPLIFIED FIWI 5G XHAUL IMPLEMENTATION

The dual-band and photonically amplified FiWi 5G Xhaul implementation is described in terms of block diagram in Fig. 7. It takes advantage of photonic and wireless technologies in a unique architecture, which consists of a broadband optical MH (link between CO and DU), followed by a dual-band wireless FH (link between DU and RRU). The novel PAA approach has been interfaced with the RoF scheme at CO, by assuming a setup in accordance to that presented in the previous Section. Both 7.5 and 28.0 GHz RF-driven signals have been launched into the 12.5-km reach MH, composed by single-mode fiber. At DU, RF_1 and RF_2 have been recovered by using a wideband photodetector (PD), amplified by the electrical amplifier 1 (EA_1) with 24 dB gain and then separated by using a diplexer. Additionally, RF_1 and RF_2 have been individually amplified using narrowband purely-electrical amplifiers (EA_2 and EA_3 with 20- and 35-dB gain, respectively), before feeding a frequency selective surface (FSS)-based dual-band parabolic antenna (DBPA) [36], [37] for simultaneous radiation. Posterior, a 10-m dual-band wireless FH has been implemented as a proof-of-concept. On the other side, the following antennas have been employed to receive the RF signals at RRU: 10 and 13-dBi gain horn antennas at 7.5 and 28.0 GHz, respectively. The received RF signals have been independently amplified by low noise amplifiers (20-dB gain EA_4 and 35-dB gain EA_5) and finally analyzed by using a vector signal analyzer (VSA). Fig. 8 displays some experimental setup photographs.

The FSS-based DBPA has been proposed by our research group as a technical solution for extremely high capacity wireless fronthauls, by means of simultaneously transmitting two frequency bands at high gain [36], [37]. Fig. 9(a) presents the antenna operational principle and its main parts, which is composed of a 60-cm diameter main reflector, two horn antennas acting as feeders in the C- and Ka-bands and an FSS-based subreflector (FSS-SR). At 7.5 GHz, the electromagnetic wave from the C-band feeder is directly reflected by the main reflector to be radiated (dashed arrow), since the designed FSS-SR is transparent to this band. On the other side, the signal from the Ka-band feeder at 28.0 GHz is reflected back to the main reflector by the FSS-SR in order to be radiated in the same direction (solid arrow) as a Cassegrain antenna. In this way, the proposed antenna consists of integrating a focal-point and a Cassegrain antenna at the same structure, enabling a dual-band and high gain simultaneous operation. Fig. 9(b) reports the FSS-SR transmission coefficient measurement, in which one might observe a 10-dB attenuation frequency range from the FSS-SR, giving rise a DPBA upper bandwidth of 4.5 GHz centered at 29.25 GHz. In the C-band, the proposed DBPA has presented 1.1 GHz bandwidth centered at 7.45 GHz. The DBPA measured gain was 30.0 and 39.4 dBi at 7.5 and 28.0 GHz, respectively.

The novel PAA technique characterization demonstrated photonically-assisted RF gain from 15 to 19 dB, without noise figure insertion, by varying the RF-driven signal power levels.

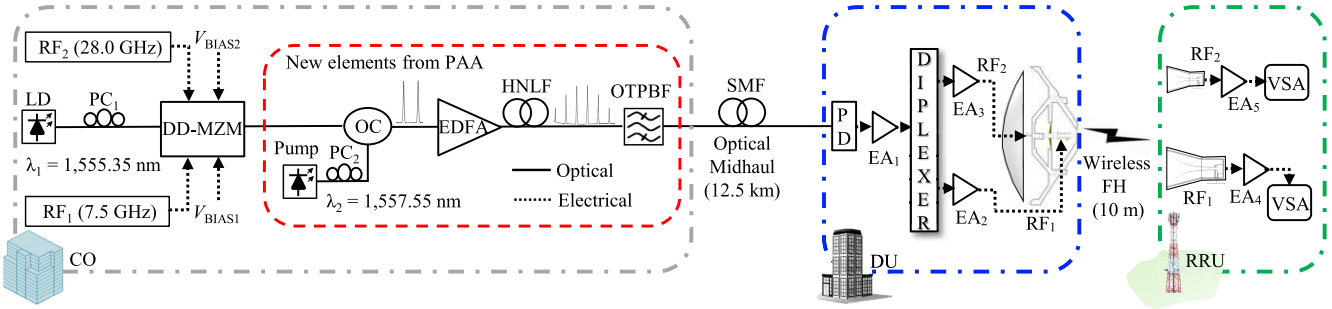

FIGURE 7. Photonics-assisted dual-band amplified fiber-wireless Xhaul architecture: MH- midhaul; EA- electrical amplifier; FH- fronthaul; VSA- vector signal analyzer; CO- central office; DU- distribution unit; RRU- remote radio unit.

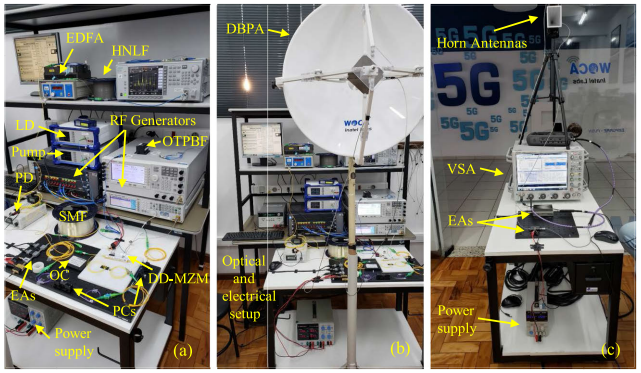

FIGURE 8. Experimental setup photographies: (a) CO and DU; (b) CO and DU front view, including the FSS-based dual-band focal point/Cassegrain parabolic antenna; (c) RRU.

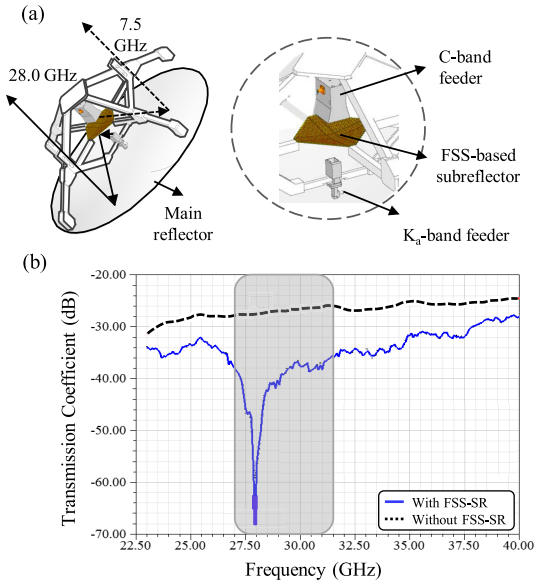

FIGURE 9. FSS-based DBPA: (a) Operational principle and its main parts; (b) Measured FSS-based subreflector transmission coefficient.

The best compromise between RF amplification and performance has been obtained for 15 dB gain with the RF-driven signal powers at 0 dBm, which implied in extremely broadband and flat gain, covering both 7.5 and 28.0 GHz

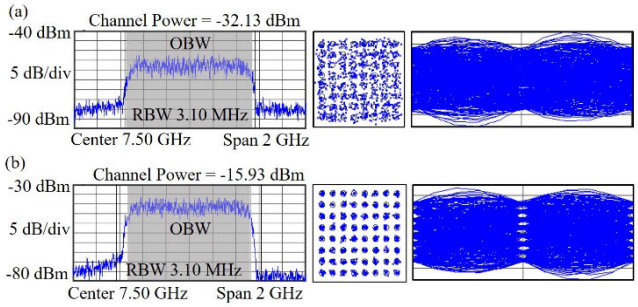

FIGURE 10. Performance of the received 7.5 GHz RF signal at 6.0 Gbit/s: (a) CRoF; (b) PAA approach.

frequencies. The CRoF system provided −47 and −59 dBm electrical power at PD output at 7.5 and 28.0 GHz, respectively, whereas the PAA approach provided −31 and −43 dBm for these frequencies. After properly amplified and separated, the signals were radiated by DBPA, giving rise to 10-m reach wireless FH.

Digital pre-distortion (DPD) has been used for enhancing the Xhaul performance. DPD consists of implementing a non-linear block with input-output amplitude and phase complementary to those resulting from the communication channel, including optical and electrical nonlinearities [38], [39]. In our implementation, electrical transmitter and receiver have been connected using Ethernet protocol to establish remote controlling, configuration and communication in a closed-loop [39]. In this way, our signal generator could pre-distort the RF generated signal for pre-compensating the communication channel, including electrical and optical components and electrical/optical and optical/electrical converters, aiming to improve the EVM_{RMS} parameter at receiver.

We have evaluated the dual-band and photonically amplified FiWi digital performance at 7.5 (RF_1) and 28.0 GHz (RF_2) in terms of EVM_{RMS} at RRU, maintaining DPD on. Fig. 10 presents a 1-GHz bandwidth 64-QAM signal at 7.5 GHz, in which one can clearly note the performance enhancement achieved by applying PAA (Fig. 10(b)) in contrast to CRoF (Fig. 10 (a)). The symbols dispersion at constellation and eye diagram opening are much less and higher,

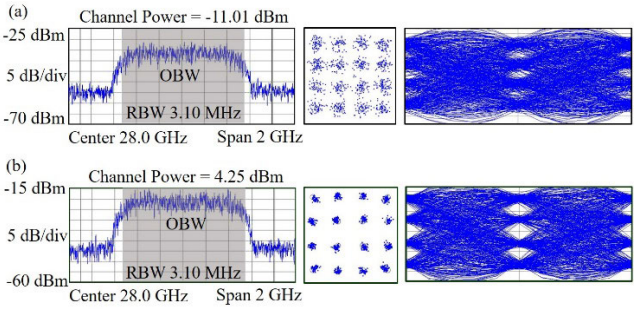

FIGURE 11. Performance of the received 28.0 GHz RF signal at 4.0 Gbit/s: (a) CRoF; (b) PAA approach.

respectively, in the PAA case. The 6.0-Gbit/s throughput transmission, over a 10-m wireless FH assisted by a 12.5 km reach optical MH, has presented 7.3% EVM_{RMS} for CRoF and only 3.4% EMV_{RMS} using the novel PAA technique, demonstrating its applicability in future mobile communication systems, including 5G. Finally, Fig. 11 reports the experimental performance comparison between CRoF (Fig. 11(a)) and PAA (Fig. 11(b)) at 28 GHz, using a 1-GHz bandwidth 16-QAM signal, resulting in 4.0 Gbit/s throughput. The PAA use implied in a significant 4.4% EVM_{RMS} improvement, from 11.6 to 6.2%. It is noticed by the symbol dispersion reduction in constellation and eye diagram opening from Fig. 10(b). The total Xhaul throughput was 10 Gbit/s by using both frequency bands.

V. CONCLUSION

A novel and innovative photonic-assisted RF amplification technique has been proposed, characterized and applied to the implementation of multiband and photonically amplified fiber-wireless Xhaul. Four-wave mixing has been stimulated by using only an optical wave and 35 m of highly nonlinear fiber in order to provide high and stable photonics-assisted RF gain at the distinct frequency bands, namely 7.5 and 28.0 GHz. In either conventional RoF and proposed systems, a dual-drive Mach-Zehnder modulator has been applied to modulate the optical carrier with both RF-driven signals. Experimental results have demonstrated 19 dB flat RF gain for both bands, with phase noise below −90 dBc/Hz at a 10-kHz offset frequency and multi-Gbit/s throughput with EVM_{RMS} improvement of up to 5.4%. Furthermore, a proof-of-concept of the proposed Xhaul has been successfully realized, enabling up to 16 Gbit/s total throughput. The novel approach has been shown seamlessly integration and potential for the envisioned 5G infrastructure, with the purpose of reducing the number of stages or even eliminating the need of purely-electrical RF amplifiers from RRU, depending on the operating frequency and cell reach. PAA has also be shown potential to significantly increase the system throughput by almost three times when compared to conventional RoF system. Our research group has recently proposed and published a multi-band architecture towards future mobile communication systems [40]. Future works regard the integration of the new photonics-assisted RF amplification technique in a FiWi system operating with diverse RF bands, including emerging flexible-waveform and multi-application 5G fiber-wireless systems.

ACKNOWLEDGMENT

The authors would like to thank engineer Masaaki Hirano from Sumitomo Industries for the donation of the HNLF used in the experiments. They also thank the technical support from Prof. Gustavo Wiederhecker from the Gleb Wataghin Institute of Physics – University of Campinas (UNICAMP).

REFERENCES

[1] *IMT Vision—Framework and Overall Objectives of the Future Development of IMT for 2020 and Beyond*, document Recommendation ITU-R M.2083-0, ITU-R, 2015, pp. 1–19.
[2] *5G; Study on Scenarios and Requirements for Next Generation Access Technologies, Version 14.2.0 Release 14*, document TR 38.913, 3GPP, 2017, pp. 1–40.
[3] D. Zhang, M. Matthe, L. L. Mendes, and G. Fettweis, "A study on the link level performance of advanced multicarrier waveforms under MIMO wireless communication channels," *IEEE Trans. Wireless Commun.*, vol. 16, no. 4, pp. 2350–2365, Apr. 2017.
[4] Y. Liu, X. Chen, Z. Zhong, B. Ai, D. Miao, Z. Zhao, J. Sun, Y. Teng, and H. Guan, "Waveform design for 5G networks: Analysis and comparison," *IEEE Access*, vol. 5, pp. 19282–19292, 2017.
[5] J. Lee, E. Tejedor, K. Ranta-aho, H. Wang, K.-T. Lee, E. Semaan, E. Mohyeldin, J. Song, C. Bergljung, and S. Jung, "Spectrum for 5G: Global status, challenges, and enabling technologies," *IEEE Commun. Mag.*, vol. 56, no. 3, pp. 12–18, Mar. 2018.
[6] H. Mehrpouyan, M. Matthaiou, R. Wang, G. Karagiannidis, and Y. Hua, "Hybrid millimeter-wave systems: A novel paradigm for hetnets," *IEEE Commun. Mag.*, vol. 53, no. 1, pp. 216–221, Jan. 2015.
[7] A. D. La Oliva, X. C. Perez, A. Azcorra, A. D. Giglio, F. Cavaliere, D. Tiegelbekkers, J. Lessmann, T. Haustein, A. Mourad, and P. Iovanna, "Xhaul: Toward an integrated fronthaul/backhaul architecture in 5G networks," *IEEE Wireless Commun.*, vol. 22, no. 5, pp. 32–40, Oct. 2015.
[8] A. Tzanakaki *et al.*, "Wireless-optical network convergence: Enabling the 5G architecture to support operational and end-user services," *IEEE Commun. Mag.*, vol. 55, no. 10, pp. 184–192, Oct. 2017.
[9] C. Lin, H. Li, J. Korhonen, J. Huang, and L. Han, "RAN revolution with NGFI (xhaul) for 5G," *J. Lightw. Technol.*, vol. 36, no. 2, pp. 541–550, Jan. 15, 2018.
[10] C. Liu, J. Wang, L. Cheng, M. Zhu, and G.-K. Chang, "Key microwave-photonics technologies for next-generation cloud-based radio access networks," *J. Lightw. Technol.*, vol. 32, no. 20, pp. 3452–3460, Oct. 15, 2014.
[11] R. Waterhouse and D. Novack, "Realizing 5G: Microwave photonics for 5G mobile wireless systems," *IEEE Microw. Mag.*, vol. 16, no. 8, pp. 84–92, Sep. 2015.
[12] X. Li, J. Yu, and G.-K. Chang, "Photonics-assisted technologies for extreme broadband 5G wireless communications," *J. Lightw. Technol.*, vol. 37, no. 12, pp. 2851–2865, Jun. 15, 2019.
[13] J. Yao, "Microwave photonics," *J. Lightw. Technol.*, vol. 27, no. 3, pp. 314–335, Feb. 1, 2009.
[14] T. Li, E. H. W. Chan, X. Wang, X. Feng, and B. Guan, "All-optical photonic microwave phase shifter requiring only a single DC voltage control," *IEEE Photon. J.*, vol. 8, no. 4, pp. 1–8, Aug. 2016.
[15] R. M. Borges, D. Mazzer, T. R. Rufino Marins, and A. C. Sodré, "Photonics-based tunable and broadband radio frequency converter," *Opt. Eng.*, vol. 55, no. 3, Dec. 2015, Art. no. 031118.
[16] A. L. M. Muniz, R. M. Borges, R. N. Da Silva, D. F. Noque, and A. Cerqueira S., "Ultra-broadband photonics-based RF front-end toward 5G networks," *J. Opt. Commun. Netw.*, vol. 8, no. 11, pp. B35–B42, Oct. 2016.
[17] F. Scotti, D. Onori, A. Bogoni, and P. Ghelfi, "Frequency-agile and filter-free wireless communication transceiver based on photonics," in *Proc. Opt. Fiber Commun. Conf. Expo. (OFC)*, San Diego, CA, USA, 2018, pp. 1–3.

[18] W. S. Wall and M. A. Foster, "Ultra-wideband gain in microwave photonic links using four-wave mixing," in *Proc. Conf. Lasers Electro-Opt. (CLEO)*, May 2012, pp. 1–2.

[19] A. C. Sodré, Jr., N. Cañas-Estrada, D. F. Noque, R. M. Borges, S. A. S. Melo, N. G. González, and J. C. R. F. Oliveira, "Photonic-assisted microwave amplification using four-wave mixing," *IET Optoelectron.*, vol. 10, no. 5, pp. 163–168, Oct. 2016.

[20] A. L. M. Muniz, D. F. Noque, R. M. Borges, A. Bogoni, M. Hirano, and A. C. Sodré, Jr., "All-optical RF amplification toward Gpbs communications and millimeter-waves applications," *Microw. Opt. Technol. Lett.*, vol. 9, pp. 2185–2189, 2017.

[21] D. F. Noque, R. M. Borges, A. L. M. Muniz, A. Bogoni, and A. Cerqueira S., Jr., "Thermal and dynamic range characterization of a photonics-based RF amplifier," *Opt. Commun.*, vol. 414, pp. 191–194, Mar. 2018, pp. 1–3.

[22] N. Peccarelli, B. James, R. Irazoqui, J. Metcalf, C. Fulton, and M. Yeary, "Survey: Characterization and mitigation of spatial/spectral interferers and transceiver nonlinearities for 5G MIMO systems," *IEEE Trans. Microw. Theory Techn.*, vol. 67, no. 7, pp. 2829–2846, Jul. 2019.

[23] E. Ruggeri, A. Tsakyridis, G. Kalfas, A. Miliou, N. Pleros, C. Vagionas, and Y. Leiba, "Fiber wireless A-RoF/IFoF uplink of 0.4Gb/s 16-QAM and 0.6Gb/s QPSK over a 32-element 60 GHz phased array antenna for 5G fronthaul networks," in *Proc. IEEE MPW*, Ottawa, ON, Canada, Oct. 2019, pp. 1–4.

[24] G. Kalfas, C. Vagionas, A. Antonopoulos, E. Kartsakli, A. Mesodiakaki, S. Papaioannou, P. Maniotis, J. S. Vardakas, C. Verikoukis, and N. Pleros, "Next generation fiber-wireless fronthaul for 5G mmWave networks," *IEEE Commun. Mag.*, vol. 57, no. 3, pp. 138–144, Mar. 2019.

[25] C. Lim, Y. Tian, C. Ranaweera, T. A. Nirmalathas, E. Wong, and K.-L. Lee, "Evolution of radio-over-fiber technology," *J. Lightw. Technol.*, vol. 37, no. 6, pp. 1647–1656, Mar. 15, 2019.

[26] R. M. Borges, T. R. R. Marins, M. S. B. Cunha, H. R. D. Filgueiras, I. F. da Costa, R. N. da Silva, D. H. Spadoti, L. L. Mendes, and A. C. Sodre, "Integration of a GFDM-based 5G transceiver in a GPON using radio over fiber technology," *J. Lightw. Technol.*, vol. 36, no. 19, pp. 4468–4477, Oct. 2018.

[27] E. Westerberg, "4G/5G RAN architecture: How a split can make the difference," *Ericsson Technol. Rev.*, vol. 93, no. 6, pp. 1–16, Jul. 2016.

[28] S. Sun, M. Kadoch, L. Gong, and B. Rong, "Integrating network function virtualization with SDR and SDN for 4G/5G networks," *IEEE Netw.*, vol. 29, no. 3, pp. 54–59, May 2015.

[29] N. McKeown, T. Anderson, H. Balakrishnan, G. Parulkar, L. Peterson, J. Rexford, S. Shenker, and J. Turner, "OpenFlow: Enabling innovation in campus networks," *ACM SIGCOMM Comput. Commun. Rev.*, vol. 38, no. 2, pp. 69–74 , Mar. 2008.

[30] V. J. Urick, M. S. Rogge, F. Bucholtz, and K. J. Williams, "Wide-band (0.045–6.25 GHz) 40 km analogue fibre-optic link with ultra-high (>40 dB) all-photonic gain," *Electron. Lett.*, vol. 42, no. 9, p. 552, 2006.

[31] H. R. D. Filgueiras, R. M. Borges, M. Caldano Melo, T. H. Brandao, and A. Cerqueira Sodre, "Dual-band wireless fronthaul using a FSS-based focal-point/cassegrain antenna assisted by an optical midhaul," *IEEE Access*, vol. 7, pp. 112578–112587, 2019.

[32] A. Cerqueira Sodre, J. M. Chavez Boggio, A. A. Rieznik, H. E. Hernandez-Figueroa, H. L. Fragnito, and J. C. Knight, "Highly efficient generation of broadband cascaded four-wave mixing products," *Opt. Express*, vol. 16, no. 4, pp. 2816–2828, 2008.

[33] S. A. S. Melo, A. R. do Nascimento, A. Cerqueira S., L. H. H. Carvalho, D. M. Pataca, J. C. R. F. Oliveira, and H. L. Fragnito, "Frequency comb expansion based on optical feedback, highly nonlinear and erbium-doped fibers," *Opt. Commun.*, vol. 312, pp. 287–291, Feb. 2014.

[34] *Group Radio Access Network; NR; User Equipment (UE) Radio Transmission and Reception; Part 1: Range 1 Standalone, Version 15.5.0 Release 15*, document TS 38.101-1, 3GPP, 2019.

[35] *5G; NR; Base Station (BS) Radio Transmission and Reception*, document 3GPP TS 38.104 version 15.2.0 Release 15, 2018.

[36] T. H. Brandão, F. Scotti, H. R. D. Filgueiras, A. A. D. C. Alves, D. Onori, S. Melo, A. Bogoni, and A. Cerqueira Sodré, "Coherent dual-band radar system based on a unique antenna and a photonics-based transceiver," *IET Radar, Sonar Navigat.*, vol. 13, no. 4, pp. 505–511, Apr. 2019.

[37] T. H. Brandão, H. R. D. Filgueiras, A. A. C. Alves, F. Scotti, S. Melo, A. Bogoni, and S. A. Cerqueira, Jr., "Dual-band system composed by a photonics-based radar and a focal-point/cassegrain parabolic antenna," *J. Microw., Optoelectron. Electromagn. Appl.*, vol. 17, no. 4, pp. 567–578, Oct. 2018.

[38] F. M. Ghannouchi, O. Hammi, and M. Helaoui, *Behavioral Modeling and Predistortion of Wideband Wireless Transmitters*. Hoboken, NJ, USA: Wiley, 2015.

[39] D.-S. Han and T. Hwang, "An adaptive pre-distorter for the compensation of HPA nonlinearity," *IEEE Trans. Broadcast.*, vol. 46, no. 2, pp. 152–157, Jun. 2000.

[40] R. M. Borges, L. A. M. Pereira, H. R. D. Filgueiras, A. C. Ferreira, M. S. B. Cunha, E. R. Neto, D. H. Spadoti, L. L. Mendes, and A. Cerqueira S., "DSP-based flexible-waveform and multi-application 5G fiber-wireless system," *J. Lightw. Technol.*, vol. 38, no. 3, pp. 642–653, Feb. 1, 2020.

EDUARDO SAIA LIMA received the B.Sc. and M.Sc. degrees from the National Institute of Telecommunications (Inatel), Brazil, in 2017 and 2019, respectively, where he is currently pursuing the Ph.D. degree in telecommunications. From 2017 to 2019, he has experience in teaching for being a tutor in electronic circuits, digital electronics, and optics communications on undergraduate courses in the Teaching Internship Program (PED) at Inatel.

RAMON MAIA BORGES received the B.Sc. degree in electrical engineering and the M.Sc. degree in telecommunications from the National Institute of Telecommunications (Inatel), in 2012 and 2015, respectively. He is currently pursuing the Ph.D. degree in electrical engineering with the Federal University of Itajubá (Unifei), Brazil. He is also a Researcher with the Radiocommunications Reference Center Project, Inatel. His fields of interest include optical communications, wireless systems, and microwave photonics.

LUIZ AUGUSTO MELO PEREIRA received the B.Sc. degree in telecommunication engineering and the M.Sc. degree in telecommunications from the National Institute of Telecommunications (Inatel), Brazil, in 2017 and 2020, respectively. He is currently pursuing the Ph.D. degree in telecommunications with the Inatel and integrates the Laboratory WOCA (Wireless and Optical Convergent Access) Research Team. His research interests include optical communications, mobile communication systems, wireless systems, and microwave photonics.

HUGO RODRIGUES DIAS FILGUEIRAS received the B.Sc. and M.Sc. degrees in telecommunications engineering from the National Institute of Telecommunications (Inatel), Brazil, in 2016 and 2018, respectively, where he is currently pursuing the Ph.D. degree in telecommunications. From 2015 to 2018, he has experience in teaching for being a Digital Transmission, Antennas and Propagation Tutor on undergraduate courses with Inatel in the Teaching Internship Program (PED), where he is currently a Researcher with the Laboratory WOCA. His fields of interests are in antennas, wireless systems, optical-wireless systems, and mobile networks.

ANTÔNIO MARCOS ALBERTI received the Ph.D. degree in electronics and telecommunications from Unicamp, Brazil, and the Ph.D. degree from the Electronics and Telecommunications Research Institute (ETRI), South Korea. He is currently an Engineer, a Professor, and the Head of the Information and Communications Technologies (ICT) Laboratory with the Instituto Nacional de Telecomunicações (Inatel), Brazil.

ARISMAR CERQUEIRA SODRÉ, JR., received the B.Sc. degree in electrical engineering from the Federal University of Bahia, Brazil, in 2001, the M.Sc. degree from the State University of Campinas (Unicamp), Brazil, in 2002, and the Ph.D. degree from Scuola Superiore Sant'Anna, Italy, in 2006. He was an Invited Researcher and a Professor from many world-recognized universities, such as the University of Oulu, in 2017, Scuola Superiore Sant'Anna, Italy, in 2015 and 2017, Danish Technical University, Denmark, in 2013, Max-Planck Institute, Germany, in 2010, and the University of Bath, U.K., in 2004, 2005, and 2007. He is currently an Associate Professor with the National Institute of Telecommunications (Inatel), Brazil, to work in the same position. Since 2009, he has been acting as a Coordinator of research and development projects on diverse areas of telecommunications, including antennas, 5G networks, radars, and microwave photonics. He has transferred 20 products to the industry and published 241 scientific articles. He holds ten patents.